Spectrally Efficient FDM: Spectrum Saving Technique for 5G?

Tongyang Xu and Izzat Darwazeh

Department of Electronic and Electrical Engineering, University College London, London, UK
Email: {t.xu, i.darwazeh}@ee.ucl.ac.uk

***Abstract*—Spectrally efficient frequency division multiplexing (SEFDM) improves spectral efficiency relative to the well known orthogonal frequency division multiplexing (OFDM). Optimal detection of SEFDM, to recover signals corrupted by inter carrier interference (ICI), has major drawbacks in the exponential growth of detection complexity with the enlargement of system size and modulation level. This poses several challenges to SEFDM practical implementations. In this work, we present and compare practicable detection algorithms for both uncoded and coded SEFDM systems. In the case of the uncoded system, we discuss a multi-band architecture termed block-spectrally efficient frequency division multiplexing (B-SEFDM) which subdivides the signal spectrum into several blocks, allowing each block to be detected separately. The other system discussed in the paper utilizes convolutional coding with an appropriate receiver comprising a fast Fourier transform (FFT) based demodulation and detection working alongside a standard Bahl-Cocke-Jelinek-Raviv (BCJR) decoder. Mathematical modelling results show the suitability of the detector for use in large size non-orthogonal multicarrier systems. In the presence of multipath frequency selective channel, system modelling results show that this coded system with 1024 sub-carriers can save up to 45% of bandwidth compared to an otherwise equivalent OFDM.**

I. Introduction

The recent success of 4G deployment and operation has led to growing interest in the system to follow, namely 5G. Even at these early stages work has started to appear aiming to define or possibly start the debate about defining 5G possible structure and services [1][2][3][4][5]. The main expectations of 5G are to achieve high-speed communications and high spectral efficiencies. In 4G standard, OFDM is the technique used in the physical layer to pack overlapping but orthogonal sub-carriers. However, OFDM is sensitive to frequency offset which may compromise orthogonality between sub-carriers. This leads to ICI and degrades the performance significantly. Since spectrum is a limited resource, techniques that can further improve spectral efficiencies, while guarantee system performance would be in high demand. In 5G standard explorations [1][2][3][4][5], non-orthogonal concepts are commonly mentioned as potential candidates for the air interface. Early application of such techniques, in multicarrier communications, can be traced back to 2003 [6] when the technique termed SEFDM was proposed. Recently, this technique, detailed in [7], was demonstrated in an optical experimental system [8], showing significant bandwidth saving with small power penalty. Spectrum saving in SEFDM is achieved by deliberately violating the orthogonality principle, which leads to non-orthogonal overlapping sub-carriers. A similar technique termed multicarrier faster than Nyquist (FTN) was proposed in [9]. This time-domain technique increases spectral efficiency by transmitting data faster than Nyquist criteria, also resulting in non-orthogonal multicarrier systems. The requirement of orthogonality is reduced and signals can be properly recovered by using appropriate detectors. Soft detection has been successfully applied to improve detection of non-orthogonal FDM in [10] and iterative detection was implemented and used for FTN in [11]. In [12], an efficient iterative soft detector was introduced and this allowed SEFDM to save 45% of bandwidth compared to OFDM.

For SEFDM, signal detection is challenged by recovering signals from interference. Sphere decoding (SD) can achieve the maximum likelihood (ML) performance with lower complexity by searching candidates within a predefined space. However, its complexity increases greatly with the enlargement of system sizes. Lower complexity SEFDM detectors like truncated singular value decomposition-fixed sphere decoding (TSVD-FSD) [13] and iterative detection-FSD (ID-FSD) [14] were proposed to recover signals from ICI at the cost of performance. Unfortunately, such detectors are all limited to small size systems because the ICI becomes severely limiting with increased number of sub-carriers.

With the aforementioned issues, a simplified detector for a large size non-orthogonal system is highly desirable. Therefore, in this paper, we investigate both uncoded [15] and coded [12] SEFDM systems and summarize efficient detection algorithms for each scenarios. Block-SEFDM is an uncoded technique to decompose the whole spectrum into several bands and recover signals in each band independently. Since each band has a limited number of sub-carriers, such system can effectively remove out-of-band interference and employ optimal detection algorithms like ML or SD in each band. Simulation results show that by using an efficient detector, performance can be improved greatly. With respect to the coded system, we prove that an FFT based soft detector can recover effectively signals from 1024 non-orthogonal sub-carriers. The soft detector allows soft information to be exchanged between an FFT detector and an outer decoder. The Turbo principle [16] is applied in this soft detector to improve the reliability of candidate solutions in each iteration. Since the FFT is a fast and standard algorithm, this detector would be practical for future hardware implementation. Simulation

5GU 2014, November 26-27, Levi, Finland

DOI 10.4108/icst.5gu.2014.258120

results show that in a frequency selective channel scenario, approximately 45% of bandwidth is saved.

II. Spectrally efficient FDM signals

Incoming complex quadrature amplitude modulation (QAM) symbols are modulated onto non-orthogonal overlapped sub-carriers to generate SEFDM symbols. For a system with N sub-carriers, the SEFDM signal can be expressed as

$$x(t) = \frac{1}{\sqrt{T}} \sum_{l=-\infty}^{\infty} \sum_{n=0}^{N-1} s_{l,n} e^{\frac{j2\pi n\alpha(t-lT)}{T}} \tag{1}$$

where Δf denotes the frequency separation between adjacent sub-carriers defined as $\Delta f = \alpha/T$, where α is the bandwidth compression factor (BCF), T is the period of one SEFDM symbol, N is the number of sub-carriers and $s_{l,n}$ is the complex QAM symbol modulated on the n^{th} sub-carrier in the l^{th} SEFDM symbol. α determines bandwidth compressions and hence bandwidth saving equals to $(1-\alpha)\times 100\%$. OFDM has $\alpha = 1$, and $\alpha < 1$ is for SEFDM.

By sampling the first SEFDM symbol at T/Q intervals where $Q = \rho N$ and $\rho \geq 1$ is the oversampling factor, the discrete SEFDM signal is expressed as

$$X[k] = \frac{1}{\sqrt{Q}} \sum_{n=0}^{N-1} s_n e^{\frac{j2\pi nk\alpha}{Q}} \tag{2}$$

where $X[k]$ is the k^{th} time sample of the first symbol of $x(t)$ in (1) with $k = [0, 1, ..., Q-1]$ and $\frac{1}{\sqrt{Q}}$ is a scaling factor. For the sake of simplification, the signal in (2) can be expressed in a matrix form as

$$X = \mathbf{F}S \tag{3}$$

where X is a Q-dimensional vector of time samples of $x(t)$ in (1), S is an N-dimensional vector of transmitted symbols and $\mathbf{F}$ is a $Q \times N$ sub-carrier matrix with elements equal to $e^{\frac{j2\pi nk\alpha}{Q}}$.

At the receiver, X is subjected to the influence of additive white Gaussian noise (AWGN) Z. After demodulating received signals with the conjugate sub-carriers $\mathbf{F}^*$, the reception process is expressed as

$$R = \mathbf{F}^*X + \mathbf{F}^*Z = \mathbf{C}S + Z_{\mathbf{F}^*} \tag{4}$$

where R is an N-dimensional vector of received statistics which is impacted by ICI, $\mathbf{C} = \mathbf{F}^*\mathbf{F}$ is an $N \times N$ correlation matrix which describes detailed information about ICI, $\mathbf{F}^*$ is the $N \times Q$ conjugate sub-carrier matrix with elements equal to $e^{\frac{-j2\pi nk\alpha}{Q}}$ for $k = [0, 1, ..., Q-1]$ and $Z_{\mathbf{F}^*}$ is the AWGN samples demodulated by the conjugate sub-carriers.

III. Uncode SEFDM and its detection

A. B-SEFDM concept and model

With the increase of signal dimensions (e.g. the number of sub-carriers), SEFDM becomes more resilient to multipath effects but unfortunately more susceptible to intercarrier interference. Sphere decoding (SD) was initially examined as a potential solution [7], however, its complexity increases rapidly with the enlargement of the system size and it is unsuitable for practical implementations. In order to alleviate the intercarrier interference, the original spectrum can be divided into several blocks. The new spectrum is illustrated in Fig. 1(c). The B-SEFDM signal [15] is then expressed as

$$X[k] = \frac{1}{\sqrt{Q}} \sum_{l_B=0}^{\frac{N}{N_B}-1} \sum_{i=0}^{N_B-1} s_{i+l_BN_B} e^{\frac{j2\pi k\alpha(i+l_B(N_B+1))}{Q}} \tag{5}$$

where N_B is the number of sub-carriers in each block, $s_{i+l_BN_B}$ is the i^{th} symbol modulated on the ${l_B}^{th}$ block. It should be noted that not all of the sub-carriers are evenly overlapped because there is a deleted sub-carrier between adjacent blocks. Therefore, the in-band BCF α in each block should be lower than the effective BCF β. The BCF transformation is provided in Table I. $N_B = 8$ is selected for the purpose of simplifying signal detections.

Table I
Effective BCF Transformation

	Sub-carrier	In-band BCF	Effective BCF
$N_B = 8$	N=16	$\alpha = 0.612$	$\beta = 0.65$
		$\alpha = 0.659$	$\beta = 0.7$
		$\alpha = 0.753$	$\beta = 0.8$
	N=32	$\alpha = 0.5943$	$\beta = 0.65$
		$\alpha = 0.64$	$\beta = 0.7$
		$\alpha = 0.7314$	$\beta = 0.8$
	N=64	$\alpha = 0.586$	$\beta = 0.65$
		$\alpha = 0.631$	$\beta = 0.7$
		$\alpha = 0.7211$	$\beta = 0.8$
	N=128	$\alpha = 0.582$	$\beta = 0.65$
		$\alpha = 0.6266$	$\beta = 0.7$
		$\alpha = 0.7161$	$\beta = 0.8$

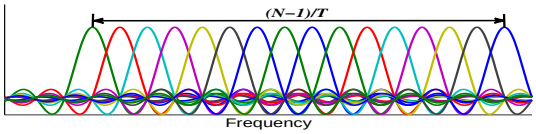

(a) OFDM Spectrum.

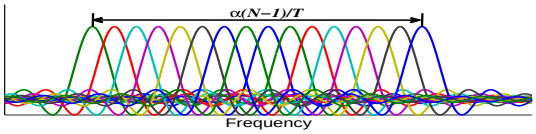

(b) SEFDM Spectrum with $\alpha = 0.8$.

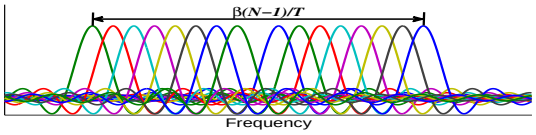

(c) B-SEFDM Spectrum with $\beta = 0.8$.

Figure 1. Spectra of 16 overlapped sub-carriers for various systems.

B. Hybrid detection

1) Iterative Detection (ID): Iterative detection [14] has a better immunity against interference. The main idea of this

detector is to recover iteratively signals which are distorted by complex interference which may be described by a matrix (e.g. correlation matrix $\mathbf{C}$). The interference is removed gradually after each iteration. The iteration process is expressed as

$$S_n = R - (\mathbf{C} - \mathbf{e})S_{n-1}, \tag{6}$$

where S_n is an N-dimensional vector of recovered symbols after n iterations, S_{n-1} is an N-dimensional vector of estimated symbols after $n-1$ iterations, $\mathbf{e}$ is an $N \times N$ identity matrix.

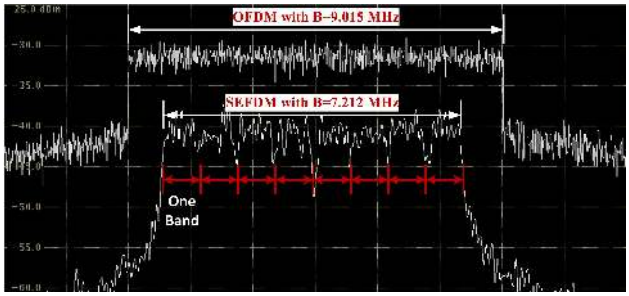

Figure 2. Experimental bandwidth comparisons of B-SEFDM ($\alpha = 0.8$) and OFDM. By transmitting the same amount of data, B-SEFDM requires bandwidth of 7.212 MHz while OFDM needs 9.015 MHz. Carrier frequency is 2 GHz, frequency span is 15 MHz and resolution bandwidth (RBW) for OFDM and B-SEFDM are 3 KHz and 60 KHz, respectively.

2) Block Efficient Detector (BED): The technique of [15] was implemented and an example of its measured signals spectrum, shown in Fig. 2, to illustrate the concept. Here, only 64 sub-carrier B-SEFDM is presented for clarity of the signal multi-band structure. In the figure, the 64 sub-carriers are divided into 8 bands; each band consists of 8 sub-carriers. At the receiver, firstly an ID detector is used to remove out-of-band interference in each sub-band. Then a 8×8 SD is adopted in each band to recover signals. Assuming the interference is cancelled out from each band, the second step of detection follows SD as

$$\tilde{S}_{BED} = \arg \min_{\tilde{S} \in O^{N_B}} \left\| \bar{R} - \bar{\mathbf{C}}\tilde{S} \right\|^2 \leq \breve{g}_{ID} \tag{7}$$

where $\breve{g}_{ID}$ is taken as the Euclidean norm between the received symbols and the initial estimates $\bar{S}$ as $\breve{g}_{ID} = \left\| \bar{R} - \bar{\mathbf{C}}\bar{S} \right\|^2$, where $\bar{\mathbf{C}}$ is an $N_B * N_B$ matrix which is a subset of $\mathbf{C}$, $\bar{S}$ is an N_B-dimensional vector of the hard decision symbols from ID detector and $\bar{R}$ is an N_B-dimensional vector of the interference cancelled received symbols. $\tilde{S}$ are final solutions and O is the constellation cardinality of 4QAM. Typically, Cholesky Decomposition is employed to simplify the calculation of Euclidean norm. The transformation is assisted by using $chol\{\bar{\mathbf{C}}^*\bar{\mathbf{C}}\} = \mathbf{L}^*\mathbf{L}$ [13], where $\mathbf{L}$ is an $N_B \times N_B$ upper triangular matrix. Therefore, (7) is transformed to an equivalent expression as

$$\tilde{S}_{BED} = \arg \min_{\tilde{S} \in O^{N}} \left\| \mathbf{L}(\hat{S} - \tilde{S}) \right\|^2 \leq \breve{g}_{ID} \tag{8}$$

where $\hat{S}$ is an N-dimensional vector of soft estimated symbols in the last iteration of ID.

C. Results

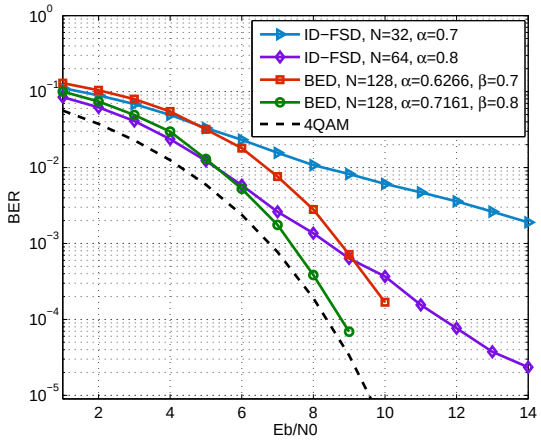

Figure 3. Performance comparisons of BED and ID-FSD for different $\alpha(\beta)$ and N with $N_B = 8$. 20 iterations are used in ID to guarantee the performance.

Fig. 3 shows that for various $\alpha(\beta)$, BED and ID-FSD perform similarly [14] for low $Eb/N0$ values, however, as $Eb/N0$ increases, the BED detector outperforms ID-FSD significantly. This performance gap is even more obvious for BED with lower bandwidth compression factor like $\alpha(\beta) = 0.7$. It should be noted that for the same bandwidth saving, the performance of a BED detector with 128 sub-carriers is even better than that of an ID-FSD detector with a smaller number of sub-carriers. Such performance improvement is attributed to the reduction of interference in the multi-band system coupled with the use of SD. Hence, one may conclude that the combination of multi-band SEFDM and BED allows practicable systems with a large number of sub-carriers and high bandwidth compression.

IV. Coded SEFDM and its Detection

A. Turbo-SEFDM concept and model

In this section, we introduce a Turbo-SEFDM architecture which maximizes the *a posteriori* probability (APP) for a given bit through a process of iteration. Fig. 5 illustrates real-time spectra of Turbo-SEFDM and Turbo-OFDM from the Tektronix Mixed Domain Oscilloscope. The white one is OFDM while the yellow one is SEFDM. It is clear seen that the bandwidth of SEFDM is compressed by 40% compared with OFDM. The complete system is depicted in Fig. 4. Detailed description can be found in work [12].

At the transmitter, a vector of uncoded bits U is encoded in the outer encoder. A coding rate $R_c = 1/2$ recursive systematic convolutional (RSC) code is employed. Feedforward polynomial and feedback polynomial are $G_1(D) = 1+D+D^2$ and $G_2(D) = 1 + D^2$, respectively [17]. The coded bits are

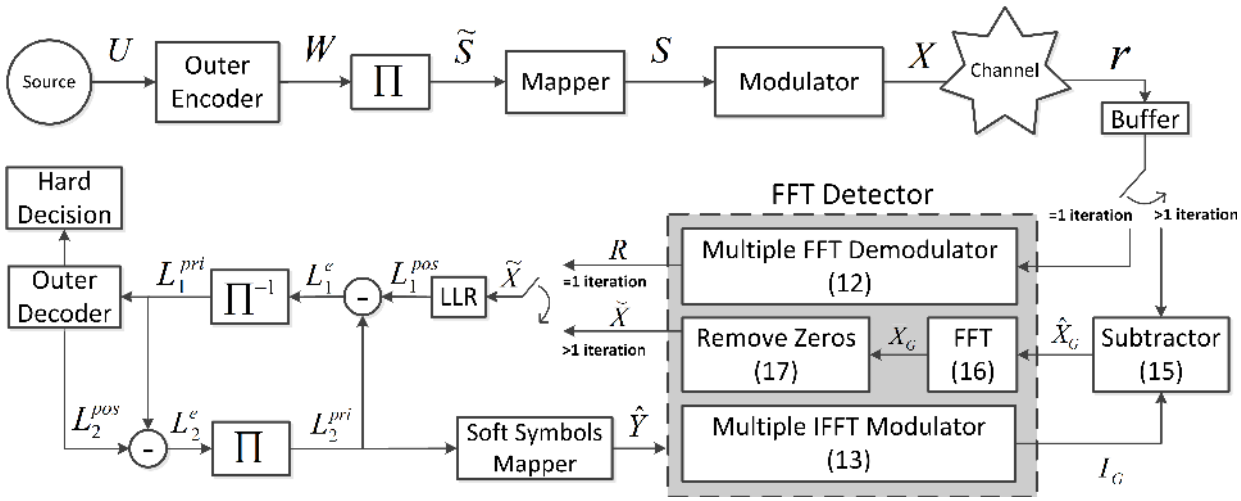

Figure 4. Block diagram of Turbo-SEFDM [12]. Equation number is (.). The block labelled $\mathbf{\Pi}$ is the interleaver and $\mathbf{\Pi^{-1}}$ represents deinterleaver.

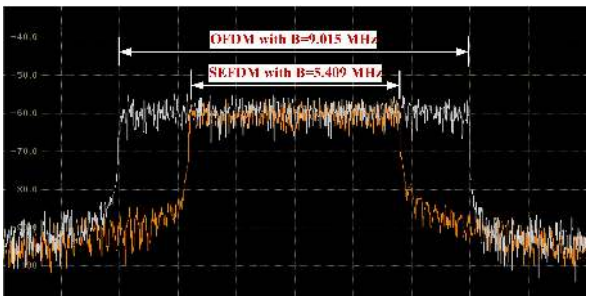

Figure 5. Experimental bandwidth comparisons of SEFDM ($\alpha = 0.6$) and OFDM. By transmitting the same amount of data, SEFDM requires bandwidth of 5.409 MHz while OFDM needs 9.015 MHz. Carrier frequency is 2 GHz, frequency span is 15 MHz and resolution bandwidth (RBW) is 3 KHz.

interleaved using a random interleaver $\mathbf{\Pi}$ with the size of 2048 information bits, and then mapped to 4QAM symbols. The SEFDM signal consists of a stream of SEFDM symbols each carrying N complex QAM symbols is obtained in the Modulator block.

At the receiver, after transmitting through a frequency selective channel, the received signals are stored in the Buffer and at the same time sent to the soft detector for signal recoveries. Demodulated signals are obtained in the Multiple FFT Demodulator, and used to generate soft information in the LLR module. The soft information is expressed in the form of log-likelihood ratios (LLR). The sign of the LLR value determines the sign of the bit, and its magnitude determines the reliability of the sign of the bit. The extrinsic information L^e is obtained by subtracting $a\ priori$ information from $a\ posteriori$ information expressed as $L^e = L_{a-posteriori} - L_{a-priori}$. After deinterleaving, the extrinsic information is delivered to the Outer Decoder as the $a\ priori$ information L_1^{pri}. The outer decoder outputs $a\ posteriori$ information L_2^{pos} which is then used to generates extrinsic information L_2^e by subtracting the $a\ priori$ information L_1^{pri}. This information is interleaved and sent back to the soft symbols mapper as the new $a\ priori$ information L_2^{pri}. Complex symbols $\hat{Y}$ are re-generated and re-modulated in order to get interference I_G. More accurate received symbols $\hat{X}_G$ are obtained in the Subtractor after removing interference. The extrinsic information is updated iteratively until the performance converges to a fixed level. Notice that in the first iteration, original received symbols r are used while in the case of more iterations, the interference cancelled symbols $\hat{X}_G$ from Subtractor are put to use.

B. Soft detector

1) Outer Decoder : SEFDM introduces ICI and therefore BCJR algorithm [18] is used to assist a detector to cancel out interference based on the Turbo principle. Detailed description of the standard BCJR decoder can be found in [18].

2) FFT Detector : The FFT detector realizes both demodulation and detection since the two functions are not activated simultaneously. The basic component in the block is a FFT element which can be easily extended to an IFFT by requiring extra computations like conjugating input complex QAM symbols and output complex results. This detector can effectively eliminate interference at the demodulation stage and prevents errors from spreading to the following decoder. From (4), the demodulation process can be expressed as

$$R[n] = \frac{1}{\sqrt{Q}} \sum_{k=0}^{Q-1} r(k) e^{\frac{-j2\pi nk\alpha}{Q}} \tag{9}$$

where $n = [0, 1, ..., N-1]$, $k = [0, 1, ..., Q-1]$. By setting $\alpha = b/c$, where b and c are both integers and $b < c$, applying the same concept in [19], (9) can be expressed as the sum of multiple FFTs as

$$R[n] = \frac{1}{\sqrt{Q}} \sum_{k=0}^{cQ-1} r^{'}(k) e^{\frac{-j2\pi nk}{cQ}} \tag{10}$$

where $r^{'}$ is a cQ-dimensional vector of symbols as

$$r^{'}(i) = \begin{cases} r_{i/b} & i \ mod \ b = 0 \\ 0 & otherwise \end{cases} \quad (11)$$

by substituting with $k = i + lc$, (10) can be rearranged and further simplified to

$$R[n] = \frac{1}{\sqrt{Q}} \sum_{i=0}^{c-1} e^{\frac{-j2\pi ni}{cQ}} \sum_{l=0}^{Q-1} r^{'}(i+lc) e^{\frac{-j2\pi nl}{Q}} \quad (12)$$

The first term in the second line in (12) is a constant factor and the second term is a Q-point FFT of the sequence $r^{'}(i+lc)$. Therefore, the demodulation of SEFDM signal can be divided into c parallel OFDM demodulation. This scheme makes it easy to generate interference to the G^{th} OFDM signal as shown in (13) with condition of $G \in [0, 1, ..., c-1]$.

$$I_G[k] = \frac{1}{\sqrt{Q}} \sum_{i=0, i\neq G}^{c-1} e^{\frac{j2\pi ik}{cQ}} \sum_{l=0}^{Q-1} Y^{'}(i+lc) e^{\frac{j2\pi lk}{Q}} \quad (13)$$

where

$$Y^{'}(i) = \begin{cases} \hat{Y}_{i/b} & i \ mod \ b = 0 \\ 0 & otherwise \end{cases} \quad (14)$$

After one iteration, the interference $I_G[k]$ is subtracted from the received discrete symbols $r[k]$ to get more reliable interference cancelled received symbols $\hat{X}_G[k]$ as

$$\hat{X}_G[k] = r[k] - I_G[k] \quad (15)$$

Notice that the interference is only removed from the G^{th} OFDM signal. Manipulation of this single OFDM signal is straightforward as shown in (16). The conjugate multiplication inside the bracket of (16) removes the complex constant factor; the operation on the exponential outside the bracket is a standard FFT.

$$\bar{X}_G[k] = \sum_{l=0}^{Q-1} [\hat{X}_G[k] e^{\frac{-j2\pi Gk}{cQ}}] e^{\frac{-j2\pi lk}{Q}} \quad (16)$$

Repeating the same process for c times, we obtain a $C \times Q$ matrix $\bar{\mathbf{X}} = [\bar{X}_0, \bar{X}_1, ..., \bar{X}_{c-1}]$ which is interpolated with zeros. Extracting data from the matrix is straightforward based on the data pattern in (11). After removing zeros, we get a single vector $\breve{X}$ composed of soft symbols as

$$\breve{x}_{i/b} = \bar{x}_i, i \ mod \ b = 0 \quad (17)$$

where $\breve{x}_{i/b}$ and $\bar{x}_i$ are the elements of vector $\breve{X}$ and matrix $\bar{\mathbf{X}}$, respectively. $\breve{X}$ are delivered back to the Turbo system to recover signals iteratively. This process continues until a converged performance is obtained.

3) LLR Calculations: A more detailed description of LLR calculations can be found in [16][20]. In this work, the log-likelihood ratio of the transmitted bit $\tilde{S}$ conditioned on the demodulation output $\tilde{X}$ is defined as

$$L(\tilde{s}|\tilde{x}) = ln \frac{P(\tilde{s} = +1|\tilde{x})}{P(\tilde{s} = -1|\tilde{x})} \quad (18)$$

The conditioned log-likelihood ratio is written as $L(\tilde{s}|\tilde{x}) = L(\tilde{s}) + L(\tilde{x}|\tilde{s})$. Thus, the above equation can be rearranged as

$$\begin{aligned} \underbrace{L(\tilde{s}|\tilde{x})}_{a-posteriori} &= ln \frac{P(\tilde{s} = +1)}{P(\tilde{s} = -1)} + ln\{ \frac{\frac{1}{\sqrt{2\pi\sigma^2}} e^{\frac{-(\tilde{x}-b)^2}{2\sigma^2}}}{\frac{1}{\sqrt{2\pi\sigma^2}} e^{\frac{-(\tilde{x}+b)^2}{2\sigma^2}}} \} \\ &= \underbrace{ln \frac{P(\tilde{s} = +1)}{P(\tilde{s} = -1)}}_{a-priori} + \underbrace{\frac{2b\tilde{x}}{\sigma^2}}_{extrinsic} \end{aligned} \quad (19)$$

where σ^2 is the noise variance and b is the fading amplitude ($b = 1$ for AWGN channels).

4) Soft Symbols Mapper: L_2^{pri} is the LLR of the bit $\tilde{s}$. Notice that two possible values of the bit $\tilde{s}$ are taken to be $+1$ and -1. Thus, the log ratio of two probabilities of the $\tilde{s}$ is defined as

$$L_2^{pri} = ln \frac{P(\tilde{s} = +1)}{P(\tilde{s} = -1)} \quad (20)$$

Taking into account that $P(\tilde{s} = +1) = 1 - P(\tilde{s} = -1)$, and taking the exponent of both sides in (20), a new expression of (20) is given by

$$e^{L_2^{pri}} = \frac{P(\tilde{s} = +1)}{1 - P(\tilde{s} = +1)} \quad (21)$$

After rearranging the above equation, it is possible to calculate bit probabilities as

$$P(\tilde{s} = +1) = \frac{1}{1 + e^{-L_2^{pri}}} \quad (22)$$

$$P(\tilde{s} = -1) = \frac{e^{-L_2^{pri}}}{1 + e^{-L_2^{pri}}}. \quad (23)$$

Given probabilities of the bit $\tilde{s}$, the expectation of $\tilde{s}$ can be calculated as $\hat{Y} = (+1) \times P(\tilde{s} = +1) + (-1) \times P(\tilde{s} = -1)$.

C. Results

The performance of Turbo-SEFDM is examined in the presence of frequency selective channel [21] as

$$\begin{aligned} h(t) = 0.8765\delta(t) - 0.2279\delta(t - T_s) + 0.1315\delta(t - 4T_s) \\ -0.4032e^{\frac{j\pi}{2}} \delta(t - 7T_s) \end{aligned} \quad (24)$$

assuming perfect channel state information (CSI) is known at the receiver. Results in Fig. 6 indicate that 4 iterations are sufficient to approach OFDM performance while saving up to 40% of bandwidth. As for the smaller $\alpha = 0.55$, with the same iteration number, it cannot reach the converged performance. This is due to the fact that too much ICI is introduced by using small bandwidth compression factors. However, this performance gap can be reduced by increasing the number of iterations. It is clear seen that the convergence is achieved by 7 iterations. Thus, considering a reasonable iteration number, in a multipath channel scenario, this new system can save up to 45% of bandwidth with slight performance degradation. It also indicates that the new detector is applicable for 1024 non-orthogonal sub-carrier SEFDM systems; the highest number of sub-carriers to be considered so far.

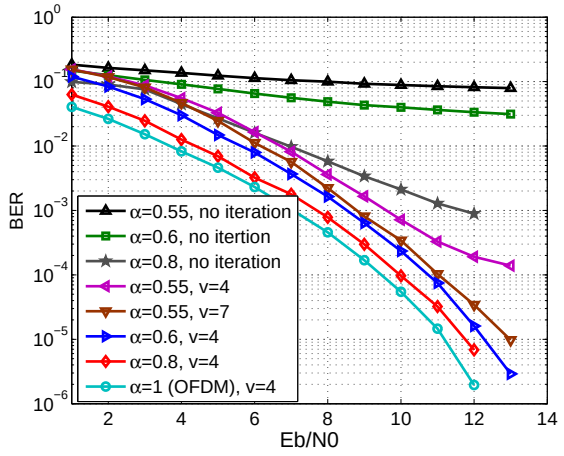

Figure 6. Performance of Turbo-SEFDM in the multipath channel (i.e. equation (24)) with N=1024 at various α. v is the number of iterations.

V. Conclusions

5G systems will aim to maximize data throughput without compromising the scarcely available spectrum. SEFDM is one such system where orthogonality is intentionally violated to improve spectral efficiency at the expense of introducing ICI. Such interference is proportional to the number of sub-carriers, which poses great challenge to SEFDM implementation and a restriction to its potential use in future systems. Therefore, large size SEFDM systems with good error performance are highly desirable and examples of these are discussed in this paper. We discuss the uncoded B-SEFDM, which reduces the detection complexity and results in good error performance by dividing the sub-carriers into several blocks. This technique is applicable to large non-orthogonal systems which in this work are tested up to 128 sub-carriers. Furthermore, a low-complexity detector, based on optimized mapping, is proposed and shown to have much improved performance when compared to other detectors used for SEFDM. Simulation shows several dB performance gain is achieved for various bandwidth compression factors. A different system is also discussed in this paper, where convolutional coding is used with a purpose designed efficient soft detector composed of FFT detector and BCJR decoder is proposed for a large size SEFDM system. A multiple FFT structure is employed to realize effectively both demodulation and detection in the FFT detector. The FFT detector works with the BCJR decoder to iteratively improve the system performance. Simulation results show that in the presence of frequency selective channel, relative to OFDM, the soft detector can save 40% of bandwidth with 1.1 dB degradation and 45% of bandwidth with a penalty of 1.6 dB in the case of 1024 non-orthogonal sub-carriers while maintaining acceptable implementation complexity.

References

[1] J. Andrews, S. Buzzi, W. Choi, S. Hanly, A. Lozano, A. Soong, and J. Zhang, "What will 5G be?" *Selected Areas in Communications, IEEE Journal on*, vol. 32, no. 6, pp. 1065–1082, June 2014.

[2] G. Wunder, P. Jung, M. Kasparick, T. Wild, F. Schaich, Y. Chen, S. Brink, I. Gaspar, N. Michailow, A. Festag, L. Mendes, N. Cassiau, D. Ktenas, M. Dryjanski, S. Pietrzyk, B. Eged, P. Vago, and F. Wiedmann, "5GNOW: non-orthogonal, asynchronous waveforms for future mobile applications," *Communications Magazine, IEEE*, vol. 52, no. 2, pp. 97–105, February 2014.

[3] A. Zakrzewska, S. Ruepp, and M. Berger, "Towards converged 5G mobile networks-challenges and current trends," in *ITU Kaleidoscope Academic Conference: Living in a converged world - Impossible without standards?, Proceedings of the 2014*, June 2014, pp. 39–45.

[4] Y. Saito, A. Benjebbour, Y. Kishiyama, and T. Nakamura, "System-level performance evaluation of downlink non-orthogonal multiple access (NOMA)," in *Personal Indoor and Mobile Radio Communications (PIMRC), 2013 IEEE 24th International Symposium on*, Sept 2013, pp. 611–615.

[5] A. Sahin, I. Guvenc, and H. Arslan, "A survey on multicarrier communications: Prototype filters, lattice structures, and implementation aspects," *Communications Surveys Tutorials, IEEE*, vol. 16, no. 3, pp. 1312–1338, Third 2014.

[6] M. Rodrigues and I. Darwazeh, "A spectrally efficient frequency division multiplexing based communications system," in *Proc. 8th Int. OFDM Workshop*, Hamburg, 2003, pp. 48 – 49.

[7] I. Kanaras, A. Chorti, M. Rodrigues, and I. Darwazeh, "Spectrally efficient FDM signals: bandwidth gain at the expense of receiver complexity," in *Communications, 2009. ICC '09. IEEE International Conference on*, 2009, pp. 1–6.

[8] I. Darwazeh, T. Xu, T. Gui, Y. Bao, and Z. Li, "Optical SEFDM system; bandwidth saving using non-orthogonal sub-carriers," *Photonics Technology Letters, IEEE*, vol. 26, no. 4, pp. 352–355, Feb 2014.

[9] J. Anderson, F. Rusek, and V. Owall, "Faster-than-Nyquist signaling," *Proceedings of the IEEE*, vol. 101, no. 8, pp. 1817–1830, 2013.

[10] N. Ahmad, S. Kamilah Syed-Yusof, N. Fisal, K. Anwar, and T. Matsumoto, "Soft-feedback MMSE equalization for non-orthogonal frequency division multiplexing (n-OFDM) signal detection," in *Smart Antennas (WSA), 2012 International ITG Workshop on*, March 2012, pp. 248–255.

[11] D. Dasalukunte, F. Rusek, and V. Owall, "An 0.8-mm^2 9.6-mw iterative decoder for faster-than-Nyquist and orthogonal signaling multicarrier systems in 65-nm CMOS," *Solid-State Circuits, IEEE Journal of*, vol. 48, no. 7, pp. 1680–1688, July 2013.

[12] T. Xu and I. Darwazeh, "A soft detector for spectrally efficient systems with non-orthogonal overlapped sub-carriers," *Communications Letters, IEEE*, vol. 18, no. 10, pp. 1847–1850, Oct 2014.

[13] S. Isam, I. Kanaras, and I. Darwazeh, "A truncated SVD approach for fixed complexity spectrally efficient FDM receivers," in *IEEE Wireless Commun. and Networking Conf.*, Mexico, WCNC, 2011.

[14] T. Xu, R. C. Grammenos, F. Marvasti, and I. Darwazeh, "An improved fixed sphere decoder employing soft decision for the detection of non-orthogonal signals," *Communications Letters, IEEE*, vol. 17, no. 10, pp. 1964–1967, 2013.

[15] T. Xu and I. Darwazeh, "Multi-band reduced complexity spectrally efficient FDM systems," in *Communication Systems, Networks Digital Signal Processing (CSNDSP), 2014 9th International Symposium on*, July 2014, pp. 982–987.

[16] J. Hagenauer, "The turbo principle: tutorial introduction and state of the art," in *Proc. Int. Symp. Turbo Codes*, Sept 1997, pp. 1–11.

[17] B. Hochwald and S. Ten Brink, "Achieving near-capacity on a multiple-antenna channel," *Communications, IEEE Transactions on*, vol. 51, no. 3, pp. 389–399, March 2003.

[18] L. Bahl, J. Cocke, F. Jelinek, and J. Raviv, "Optimal decoding of linear codes for minimizing symbol error rate (corresp.)," *Information Theory, IEEE Transactions on*, vol. 20, no. 2, pp. 284–287, Mar 1974.

[19] P. Whatmough, M. Perrett, S. Isam, and I. Darwazeh, "VLSI architecture for a reconfigurable spectrally efficient FDM baseband transmitter," *Circuits and Systems I: Regular Papers, IEEE Transactions on*, vol. 59, no. 5, pp. 1107–1118, May 2012.

[20] L. Hanzo, T. H. Liew, B. L. Yeap, R. Y. S. Tee, and S. X. Ng, *Turbo coding, turbo equalization and space-time coding: EXIT-chart-aided near-capacity designs for wireless channels*, 2nd ed. John Wiley and Sons, Ltd, 2011.

[21] X. Wang, P. Ho, and Y. Wu, "Robust channel estimation and ISI cancellation for OFDM systems with suppressed features," *Selected Areas in Communications, IEEE Journal on*, vol. 23, no. 5, pp. 963–972, May 2005.